Journal of Geomine (2023), 1(1), 22-29
DOI: 10.22077/jgm.2023.6392.1005

Estimation of passive earth pressure against a battered rigid retaining wall in cohesive-frictional backfill

Hassan Sarfaraz[1], Mohammad Hossein Khosravi[1,2], Thirapong Pipatpongsa[3], Gholamreza Saedi[4]

Recived: 2023 May 20, Revised: 2023 Jul. 12, Online Published: 2023 Jul. 15

ABSTRACT

Typically, the earth pressure against rigid retaining walls is calculated using the classical Coulomb and Rankine theories resulting in a linear distribution. However, many experimental results have shown that the earth pressure distribution on a wall is nonlinear due to the arching phenomenon. The concept of arching phenomenon in soil was realized experimentally by Terzaghi using some trap door tests. He observed that when a part of the support yields, the soil on that part moves towards the yielding support. The relative movement of the soil leads to the mobilization of the frictional resistance in the soil, and as a result, a part of the weight of the yielded area is transferred to the adjacent stable areas. Considering this phenomenon and the limit equilibrium condition, a theoretical solution is proposed to predict the vertical and horizontal passive earth pressures of cohesive soils behind inclined retaining structures under translational movement. Parametric analyses investigate the influence of some parameters, including surcharge load, cohesion, internal friction angle, the interaction between the soil-wall, and wall inclination on the distribution of passive earth pressure. Finally, the resultant passive lateral thrust on the wall and its application height are compared with the well-known classical theories of Coulomb and Rankine.

KEYWORD

Retaining wall, arching effect, theoretical solution, passive earth pressure

SYMBOL LIST

z	vertical distance from the surface
σ_1 , σ_3	major, and minor principal stresses
σ_{ph}	passive horizontal earth pressure
P_h	resultant horizontal force
M_h	moment of the horizontal stress
h_p	application point of resultant thrust force
σ_{nw}	normal stress along the wall
τ_w	shear stress along the wall
α	angle of the failure plane
γ	unit weight
c	cohesion
φ	internal friction angle
δ	interface friction angle
H	wall height
Q	uniform surcharge
R	radius of σ_1 trajectory
θ	inclined angle of σ_3 along the wall
ψ	inclined angle of σ_3 at any point
β	angle of wall batter

I. INTRODUCTION

The studies on the interaction between backfill soil and retaining walls can be divided into two main groups, active and passive. This study is limited to the translational passive mode of wall movement. A schematic view of the passive failure wedge behind the wall and its corresponding failure surface is shown in Fig. 1. In general, the earth pressure against the retaining wall is determined by the weight of the failure wedge and the shearing resistance of soil along the failure surface.

Several classic theories investigated passive earth pressure, including those by Coulomb (1776) and Rankine (1857). In these methods, the pressure distribution is linear. Conversely, some physical (Fang et al., 1994, 2002; Xu et al., 2002, 2022; O'Neal and Hagerty 2011; Khosravi et al., 2013; Ying et al., 2016; Jun-wu et al., 2019) and numerical simulations (Liu et al., 2018; Chen et al., 2020, 2021, 2022; Kejia et al., 2021; Lu et al., 2021; Jiang et al., 2022) indicated that distribution of earth pressure of backfill against an unsmooth wall is non-linear that this issue is related to soil arching effect. Firstly, this phenomenon is presented by Terzaghi (1943). Then, it was used in approaches for calculating passive earth pressure (Dalvi and Pise 2012; Cao et al. 2019). Using the pseudo-static approach, Pain et al. (2017) proposed an euation to compute the seismic earth pressure of

[1] School of Mining Engineering, College of Engineering, University of Tehran, Iran, [2] Department of Mining Engineering, Faculty of Engineering, University of Birjand, Iran, [3]Department of Urban Management, Kyoto University, Kyoto, Japan, [4] Millennium Iranian Construction and Trading Company, Tehran, Iran

✉ M.H. Khosravi: mh.khosravi@birjand.ac.ir

granular backfills. Their method is so sensitive respected to the height of the wall. So that at a wall height higher than one meter, the pressure is negative in the upper zone of the wall. Though, the pressure should be positive at any height of the wall, which can be considered one of the defects of this method. Alqarawi et al. (2021) established a formula for predicting passive earth pressure of inclined granular soil by the development of Terzaghi's (1943) log-spiral approach. Besides, these reseachers performed some experimental tests to examine failure surface.

Researches for predicting the pressure of cohesive-frictional soil are not numerous. Cai et al. (2017) derived a method to estimate the passive earth pressure of cohesive backfill behind vertical retaining walls. They assumed the symmetric curve for the trajectory of major principal stress was assumed in their study. However, researchers such as (Dalvi and Pise, 2012; Cao et al., 2019; Ghaffari and Shahir, 2019) considered an asymmetric curve for the aforementioned stress trajectory. In a completely rough face, the method of Cai et al. (2017) does not achieve appropriate results and the failure line positions along the wall are considered a shortcoming of their approach. Additionally, the pressure is overestimated in the lower zone of the wall, which is a further deficiency of their method. Ghaffari and Shahir (2019) offered an analytical method to compute the passive earth pressure of cohesive backfill against the retaining wall. However, their study was limited to vertical walls.

In this research, a comprehensive analytical solution is proposed in which the limitations of previous studies such as soil cohesion and wall batter are covered.

II. PROPOSED METHOD

The detailed analytical solution for computing the lateral passive earth pressure against an inclined rigid retaining wall is described in this section. As shown in Fig. 2, the failure surface behind the wall is assumed linear with an inclination angle of α=45-φ/2. In addition, following the theory of soil arching, σ_1 and σ_3, respectively, are assumed tangential and perpendicular to a concave arch. The trajectory of major principal stress continues under passive conditions.

The passive lateral earth pressure on an arbitrary differential element inside the backfill soil can be obtained using the following equation:

$$\sigma_{ph} = \sigma_1 \sin^2\psi + \sigma_3 \cos^2\psi \quad (1)$$

where σ_{ph} is the passive lateral earth pressure, σ_1 and σ_3 are principal stresses, and ψ is the inclined angle of σ_3. Considering cohesive soil under passive condition, the following equation can be written.

$$\sigma_1 = k_p\sigma_3 + \left(k_p - 1\right)\frac{c}{\tan\varphi} \quad (2)$$

In which k_p is developed by Rankine (1857).

$$k_p = \frac{1+\sin\varphi}{1-\sin\varphi} \quad (3)$$

With the substitution of Eq. (2) in Eq. (1), the lateral passive earth pressure is achieved as follows.

$$\sigma_{ph} = \sigma_3\left(\cos^2\psi + k_p \sin^2\psi\right) + \frac{c}{\tan\varphi}\sin^2\psi\left(k_p - 1\right) \quad (4)$$

Furthermore, the pressure normal to the wall is computed as:

$$\sigma_{pnw} = \sigma_3\left(\cos^2(\theta-\beta) + k_p \sin^2(\theta-\beta)\right) + \frac{c}{\tan\varphi}\sin^2(\theta-\beta)\left(k_p - 1\right) \quad (5)$$

Considering the first stress invariant,

$$I_1 = \sigma_1 + \sigma_3 = \sigma_{pv} + \sigma_{ph} \quad (6)$$

Substituting Eq.s (2) and (4) in Eq. (6) resulted in the following equation for σ_{pv}:

$$\sigma_{pv} = \sigma_3\left(\sin^2\psi + k_p \cos^2\psi\right) + \frac{c}{\tan\varphi}\cos^2\psi\left(k_p - 1\right) \quad (7)$$

According to Eq.s (4) and (7), lateral and vertical stresses along the differential element are functions of ψ, indicated in Fig. 2. The value of ψ changes from θ (along the wall) to 90 (at the slip surface). The θ value is a function of soil friction angle (ϕ), wall-soil interface friction angle (δ), and the wall batter (β), as defined by

$$\theta = \left[\frac{\pi}{2} - \frac{1}{2}\arcsin\left(\frac{\sin\delta}{\sin\varphi}\right) - \frac{\delta}{2}\right] + \beta \quad (8)$$

As indicated in Fig. 2, by writing the vertical differential, the following equation can be obtained.

$$dv = \sigma_v dA = \left[\sigma_3\left(\sin^2\psi + k_p \cos^2\psi\right) + \frac{c}{\tan\varphi}\cos^2\psi\left(k_p - 1\right)\right] R \sin\psi \, d\psi \quad (9)$$

The average vertical stress is achieved by dividing the total vertical force by the width of the differential element (L).

$$\overline{\sigma_v} = \frac{V}{L} = \frac{1}{R\cos\theta}\int_\theta^{\pi/2} dv \quad (10)$$

$$\overline{\sigma_v} = \int_\theta^{\pi/2}\sigma_3\left(\sin^2\psi + k_p\cos^2\psi\right)\frac{\sin\psi}{\cos\theta}d\psi + \int_\theta^{\pi/2}\frac{c}{\tan\varphi}\cos^2\psi\left(k_p - 1\right)\frac{\sin\psi}{\cos\theta}d\psi \quad (11)$$

$$\overline{\sigma_v} = \sigma_3\left(1 - \frac{1-k_p}{3}\cos^2\theta\right) + \frac{c(k_p-1)}{3\tan\varphi}\cos^2\theta \quad (12)$$

Reordering Eq. (12) for the minor principal stress, the following equation can be obtained.

$$\sigma_3 = \frac{3\overline{\sigma_v} - \frac{c(k_p-1)}{\tan\varphi}\cos^2\theta}{3-(1-k_p)\cos^2\theta} \quad (13)$$

Substituting Eq. (13) in Eq. (5), the normal passive earth pressure against the wall can be achieved.

$$\sigma_{pnw} = \frac{3\left(\cos^2(\theta-\beta)+k_p\sin^2(\theta-\beta)\right)}{3-(1-k_p)\cos^2\theta}\left(\overline{\sigma_v} - \frac{c(k_p-1)}{3\tan\varphi}\cos^2\theta\right) + \frac{c(k_p-1)}{\tan\varphi}\sin^2(\theta-\beta) \quad (14)$$

Considering the cohesion, by separating Eq. (14) into two portions, it can be simplified as:

$$\sigma_{pnw} = k_{pnw}\overline{\sigma_v} + m \quad (15)$$

where,

$$k_{pnw} = \frac{\sigma_{pnw}}{\overline{\sigma_v}} = \frac{3\left(\cos^2(\theta-\beta)+k_p\sin^2(\theta-\beta)\right)}{3-(1-k_p)\cos^2\theta} \quad (16)$$

$$m = k_{pnw}\frac{-c(k_p-1)}{3\tan\varphi}\cos^2\theta + \frac{c(k_p-1)}{\tan\varphi}\sin^2(\theta-\beta) = \frac{c(1-k_p)}{\tan\varphi}\left(\frac{k_{pnw}\cos^2\theta}{3} - \sin^2(\theta-\beta)\right) \quad (17)$$

The differential element of the soil behind the wall and the stresses acting on it are indicated in Fig. 3.

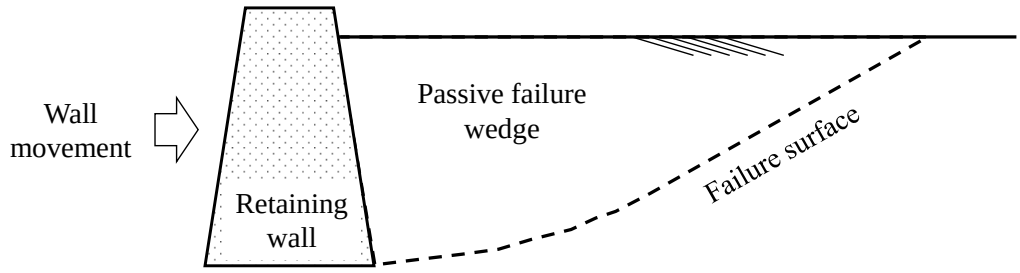

Fig. 1. Passive failure wedge behind the wall and its corresponding failure surface

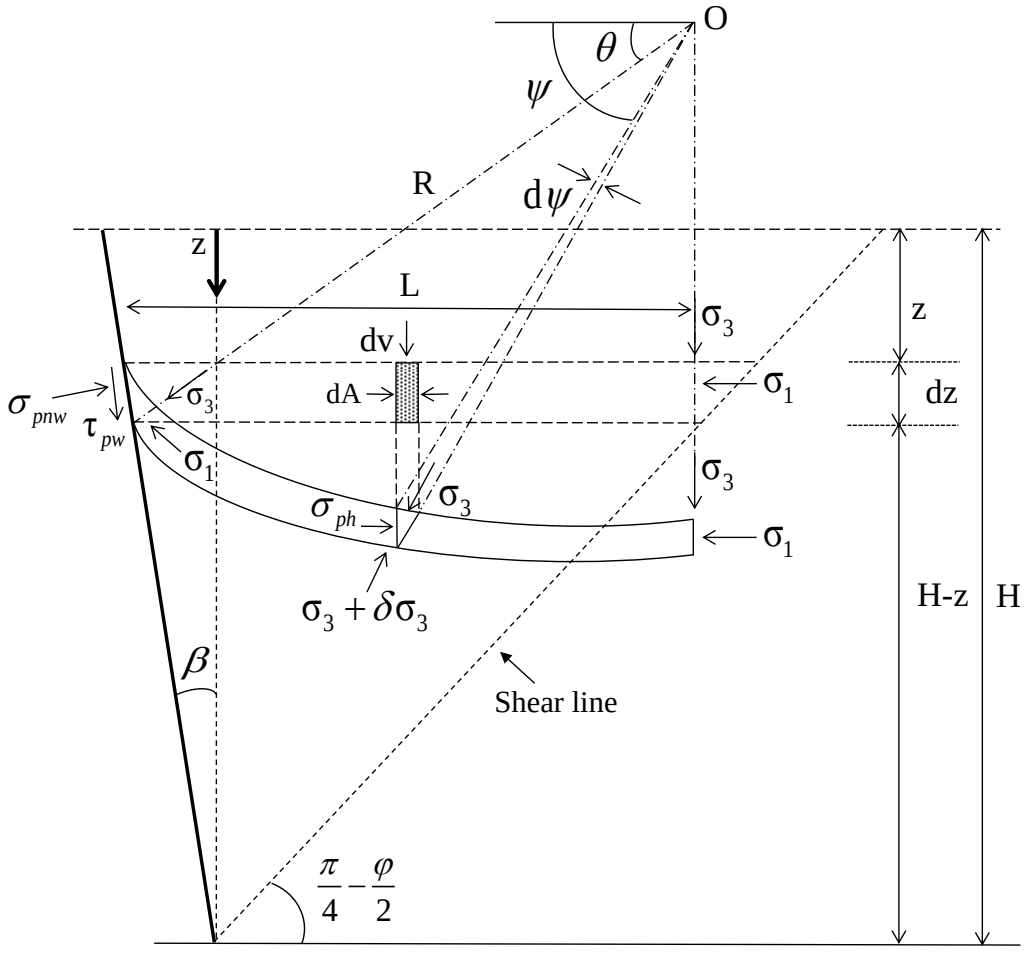

Fig. 2. Stresses on a differential element

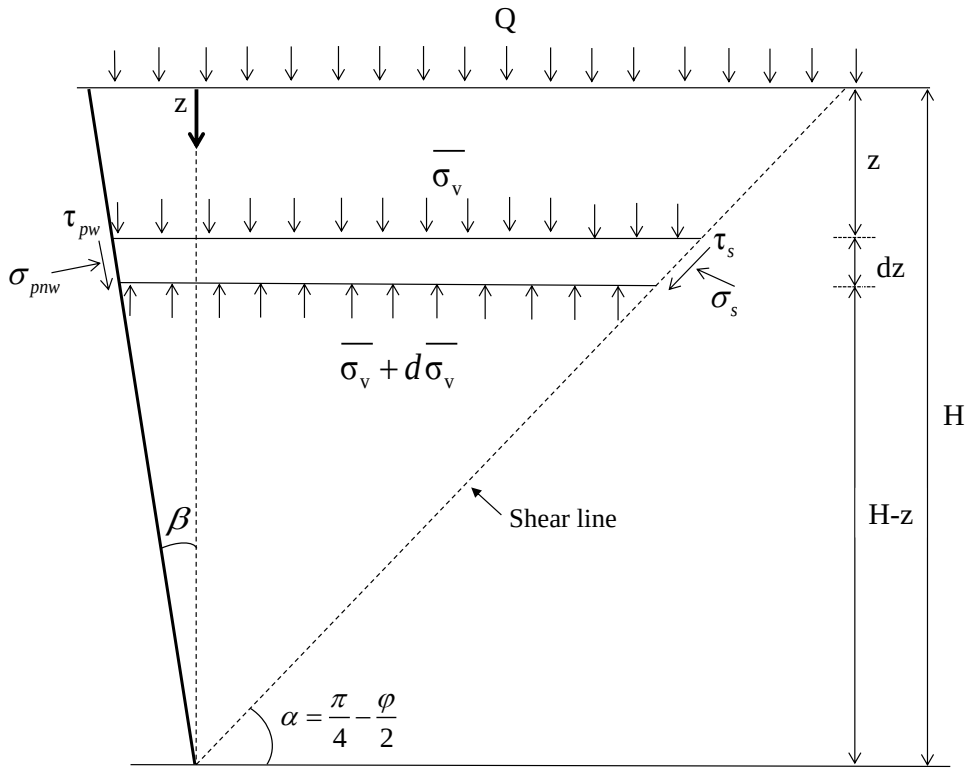

Fig. 3. The free-body diagram of the differential element

The contribution of stresses applied on the slip surface was considered in the presented formulation. Thus, taking the force equation along the vertical direction leads to the following equation:

$$\frac{d(\overline{\sigma_v} l)}{Ldz} + \frac{-\tau_{pw} - \tau_s + \sigma_s \cot\alpha + \sigma_{pnw} \tan\beta}{L} = \gamma \quad (18)$$

where,

$$L = (H - z)(\cot\alpha + \tan\beta) \quad (19)$$

The shear and normal stresses on the slip plane can be computed as follows:

$$\sigma_s = \frac{(k_p - 1)\cos^2\varphi}{2\sin\varphi}\left(\sigma_3 + \frac{c}{\tan\varphi}\right) - \frac{c}{\tan\varphi} \quad (20)$$

$$\tau_s = c + \sigma_s \tan\varphi = \frac{(k_p - 1)\cos\varphi}{2}\left(\sigma_3 + \frac{c}{\tan\varphi}\right) \quad (21)$$

Using the Eq.s (5, 15-17), σ_s and τ_s are calculated as:

$$\sigma_s = \frac{(k_p - 1)\cos^2\varphi k_{pnw}}{2\sin\varphi\left(\cos^2(\theta-\beta) + k_p \sin^2(\theta-\beta)\right)}\overline{\sigma_v} + \frac{(k_p - 1)\cos^2\varphi}{2\sin\varphi}\frac{c\left[1 + (1 - k_p)\left(\frac{k_{pnw}\cos^2\theta}{3} - \sin^2(\theta-\beta)\right)\right]}{\tan\varphi\left(\cos^2(\theta-\beta) + k_p \sin^2(\theta-\beta)\right)} - \frac{c}{\tan\varphi} \quad (22)$$

$$\tau_s = \frac{(k_p - 1)\cos\varphi k_{pnw}}{2\left(\cos^2(\theta-\beta) + k_p \sin^2(\theta-\beta)\right)}\overline{\sigma_v} + \frac{(k_p - 1)\cos\varphi}{2\tan\varphi}\frac{c\left[1 + (1 - k_p)\left(\frac{k_{pnw}\cos^2\theta}{3} - \sin^2(\theta-\beta)\right)\right]}{\left(\cos^2(\theta-\beta) + k_p \sin^2(\theta-\beta)\right)} \quad (23)$$

Correspondingly.

In addition, τ_{pw} can be achieved as:

$$\tau_{pw} = k_{pnw} \tan\delta\, \overline{\sigma_v} + \frac{c\tan\delta\left[1 + (1 - k_p)\left(\frac{k_{pnw}\cos^2\theta}{3} - \sin^2(\theta-\beta)\right)\right]}{\tan\varphi} \quad (24)$$

The following differential equation can be achieved by substituting Eq.s (14, 21-24) into Eq. (17).

$$\frac{d\overline{\sigma_v}}{dz} - \frac{\overline{\sigma_v}}{H - z} + \frac{A'\overline{\sigma_v} + B'}{(H - z)(\cot\alpha + \tan\beta)} = \gamma \quad (25)$$

In which:

$$A' = A_1 + A_2 + A_3 + A_4 \quad (26)$$

$$A_1 = -k_{pnw} \tan\delta \quad (27)$$

$$A_2 = \frac{(1-k_p)\cos\varphi k_{pnw}}{2(\cos^2(\theta-\beta)+k_p\sin^2(\theta-\beta))} \quad (28)$$

$$A_3 = \frac{(k_p-1)\cos^2\varphi\cot\alpha k_{pnw}}{2\sin\varphi(\cos^2(\theta-\beta)+k_p\sin^2(\theta-\beta))} \quad (29)$$

$$A_4 = k_{pnw}\tan\beta \quad (30)$$

$$B' = B_1 + B_2 + B_3 + B_4 \quad (31)$$

$$B_1 = -\frac{c\tan\delta\left[1+(1-k_p)\left(\frac{k_{pnw}\cos^2\theta}{3}-\sin^2(\theta-\beta)\right)\right]}{\tan\varphi} \quad (32)$$

$$B_2 = \frac{(1-k_p)\cos\varphi}{2\tan\varphi}\frac{c\left[1+(1-k_p)\left(\frac{k_{pnw}\cos^2\theta}{3}-\sin^2(\theta-\beta)\right)\right]}{(\cos^2(\theta-\beta)+k_p\sin^2(\theta-\beta))} \quad (33)$$

$$B_3 = \frac{(k_p-1)\cos^2\varphi\cot\alpha}{2\sin\varphi}\frac{c\left[1+(1-k_p)\left(\frac{k_{pnw}\cos^2\theta}{3}-\sin^2(\theta-\beta)\right)\right]}{\tan\varphi(\cos^2(\theta-\beta)+k_p\sin^2(\theta-\beta))} - \frac{c\cot\alpha}{\tan\varphi} \quad (34)$$

$$B_4 = \frac{c(1-k_p)\tan\beta}{\tan\varphi}\left(\frac{k_{pnw}\cos^2\theta}{3}-\sin^2(\theta-\beta)\right) \quad (35)$$

Now, Eq. (25) can be simplified as:

$$\frac{d\overline{\sigma_v}}{dz} = \gamma + \frac{\lambda\overline{\sigma_v}-B}{H-z} \quad (36)$$

where,

$$\lambda = 1 - \frac{A'}{\cot\alpha+\tan\beta} \quad (37)$$

$$B = \frac{B'}{\cot\alpha+\tan\beta} \quad (38)$$

By applying the boundary condition $\overline{\sigma_v}=Q$ at z=0 to Eq. (36), the average vertical stress can be computed as follows:

$$\overline{\sigma_v} = \left(Q+\frac{\gamma H}{1+\lambda}\right)\left(1-\frac{z}{H}\right)^{-\lambda} - \frac{\gamma(H-z)}{1+\lambda} + \frac{B}{\lambda}\left(1-\left(1-\frac{z}{H}\right)^{-\lambda}\right) \quad (39)$$

By substituting Eq. (39) into Eq. (15), the passive normal earth pressure against the wall can be obtained as follows.

$$\sigma_{pnw} = k_{pnw}\left[\left(Q+\frac{\gamma H}{1+\lambda}\right)\left(1-\frac{z}{H}\right)^{-\lambda} - \frac{\gamma(H-z)}{1+\lambda} + \frac{B}{\lambda}\left(1-\left(1-\frac{z}{H}\right)^{-\lambda}\right)\right] + \frac{c(1-k_p)}{\tan\varphi}\left(\frac{k_{pnw}\cos^2\theta}{3}-\sin^2(\theta-\beta)\right) \quad (40)$$

Finally, the lateral pressure can be achieved from the vector addition of the pressure normal to the wall and the shearing stress acting tangentially along the wall face.

$$\sigma_{p_h} = \cos(\delta-\beta)\sqrt{{\sigma_{pnw}}^2 + {\tau_{pw}}^2} \quad (41)$$

III. PARAMETRIC STUDY

A. BACKFILL INTERNAL FRICTION

The distribution of passive earth pressure along the wall height for various internal friction angles is plotted in Fig. 4. The backfill specifications are γ=15 kN/m^3, Q=0.25γH, c=0.1γH, δ=0.8φ, β=10^0. As observed in Fig., the horizontal earth pressure has a nonlinear distribution, except for frictionless backfill soils. In addition, by increasing the internal friction, the earth pressure against the wall increased, especially at the toe of the wall.

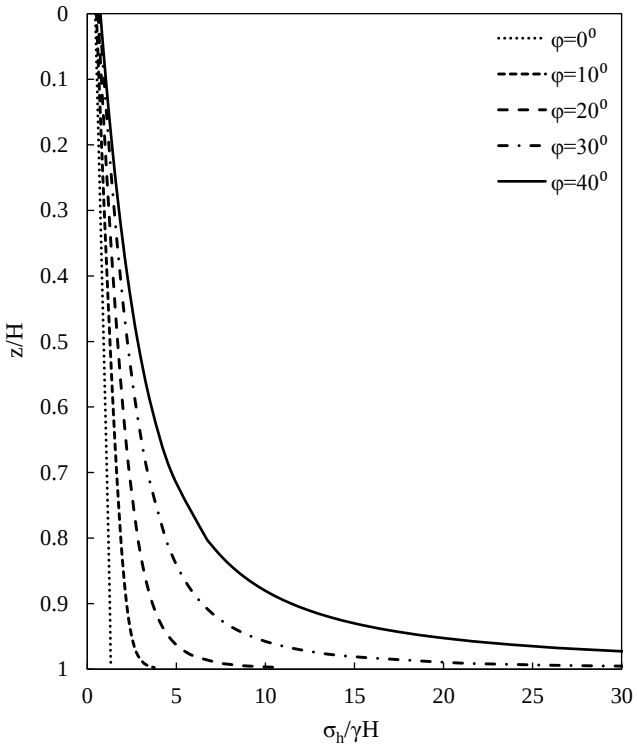

Fig. 4. The influence of φ on σ_h

B. SOIL-WALL INTERFACE FRICTION

The influence of soil-wall interface friction on the earth pressure is illustrated in Fig. 5, where the properties of γ=15 kN/m^3, c=0.1γH, Q=0.25γH, φ=30^0, β=10^0. According to this Fig., increasing the interface friction from 0 to 0.75φ resulted in a significant increase at the lower zone of the wall. It is noticeable that the earth pressure against the wall is reduced along with the wall height for a fully rough wall face.

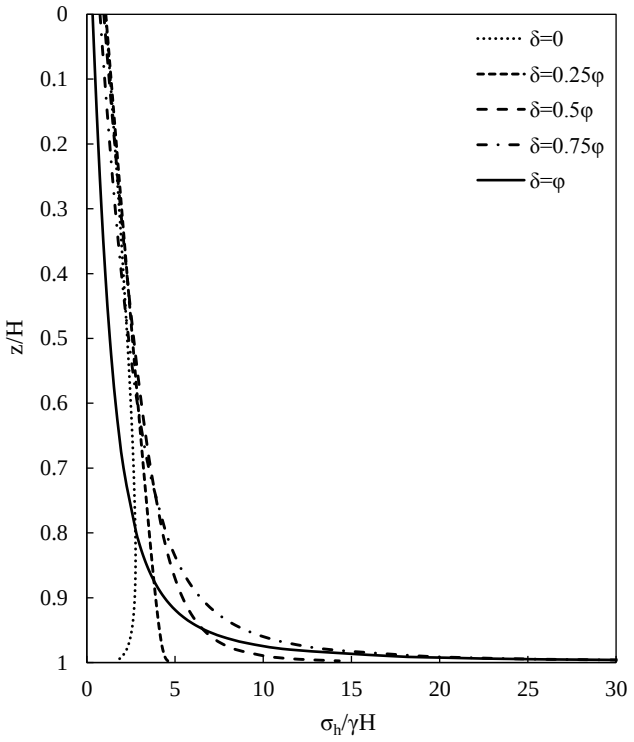

Fig. 5. The influence of δ on σ_h

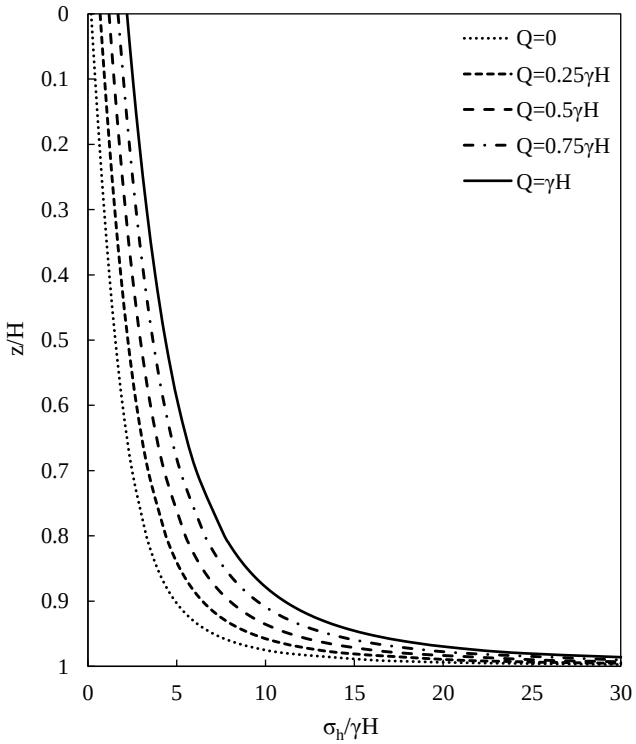

Fig. 6. The influence of Q on σ_h

C. SURCHARGE PRESSURE

The influence of surcharge on the distribution of passive horizontal earth pressure is shown in Fig. 6. The input parameters for plotting these graphs are γ=15 kN/m^3, c=0.1γH, φ=30^0, δ=0.8φ, β=10^0. As expected, increasing the surcharge has no influence on the shape of pressure distribution but results in an increase in the pressure values.

D. BACKFILL COHESION

The effect of backfill cohesion on the earth pressure is presented in Fig. 7, where used specifications are γ=15 kN/m^3, Q=0.25γH, φ=30^0, δ=0.8φ, β=10^0, and cohesion of soil varied from 0 to 0.4γH. As shown in Fig. 7, increasing the backfill soil cohesion leads to increasing the lateral earth pressure, everywhere along with the height of the wall.

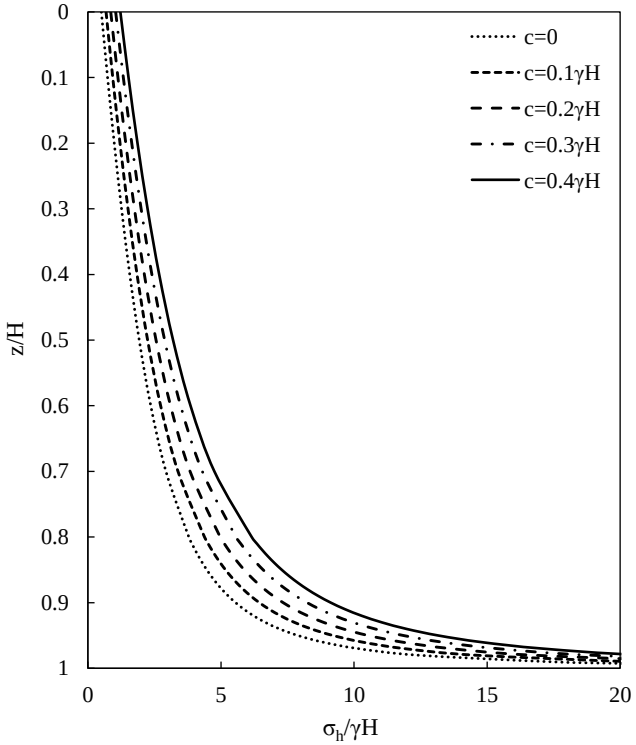

Fig. 7. The influence of cohesion on σ_h

E. WALL BATTER

The effect of the wall batter on the earth pressure distribution is indicated in Fig. 8. The used parameters are γ=15 kN/m^3, c=0.1γH, Q=0.25γH, φ=30^0, and δ=0.5φ, with a wall inclination varying from 0^0 to 20^0. According to this Fig. 8, increasing the wall batter has a reverse influence on the lateral earth pressure at the lower portion of the wall. However, it does not affect the upper portion of the wall.

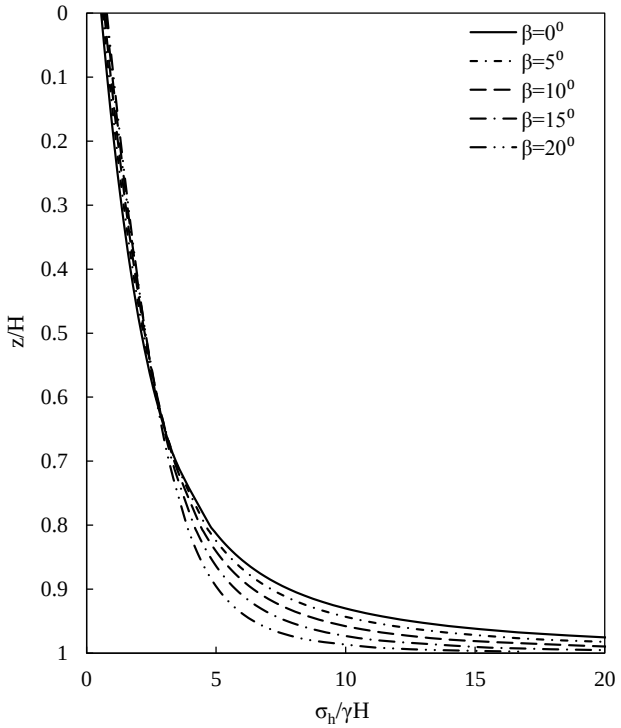

Fig. 8. The influence of β on σ_h

IV. DISCUSSION

By integrating σ_{ph} along the vertical direction, the resultant lateral force can be calculated.

$$P_h = \int_0^H \sigma_{ph}\, dz \tag{42}$$

Besides, the moment of horizontal stress around the toe of the wall can be computed as:

$$M_h = \int_0^H \sigma_{ph}\,(H - z) dz \tag{43}$$

The application point of P_h can be achieved by dividing Eq. (43) by Eq. (42).

$$h_p = \frac{M_h}{P_h} \tag{44}$$

The values of P_h and h_p for granular soil behind inclined walls are shown in Fig. 9. The classic theories are also plotted in Fig. 9. Taylor (1948) extended the theory of Rankine (1857) to the battered retaining wall, where Rankine method is applied to the virtual plane. The values of P_h, in Fig. 9 (a), are shown as a normalized ratio of K_{ph}.

$$K_{p_h} = \frac{P_h}{0.5\gamma H^2} \tag{45}$$

According to Fig. 9 (a), the results of the suggested theoretical approach are lower than Coulomb (1776) theory. According to Fig. 19 (b), h_p=H/3 in the theories of Coulomb (1776) and Rankine (1857), while in the proposed method, the application point of thrust force changes with the wall batter, and it increases with rising the wall batter.

V. CONCLUSIONS

The arching effect plays a significant role in the retaining wall design in the passive earth pressure distribution. Considering this phenomenon, an equation is proposed to predict the horizontal earth pressure behind rigid retaining walls. As pre-existing methods are limited to granular soil or non-batter walls, backfill cohesion and wall inclination are taking account in the proposed formulations. The conclusions that can be drawn from this work are as follows:

1. The earth pressure distribution is curvilinear, and the arching effect is completely removed for the smooth wall. In this case, the shape of the pressure distribution is linear.
2. Increasing the strength properties of the backfill soil, including cohesion and internal friction, increases in the earth pressure against the wall.
3. Increasing the surcharge on the backfill increases the earth pressure against the wall.
4. Increasing the wall batter resulted in a decrease in the earth pressure at the lower zone of the wall, while no significant pressure changes were observed at the upper portion.
5. Rising the wall batter resulted in a decline in the arching effect at the lower area of the wall.
6. The application height of the lateral thrust on the wall is significantly lower than the values predicted by the classical theories of Coulomb and Rankine. This is due to the soil arching effect behind the wall.
7. The resultant lateral thrust predicted by this study is higher than Rankine but lower than Coulomb predictions. The reason for the Rankine's underestimation is the neglect of wall friction in his theory.

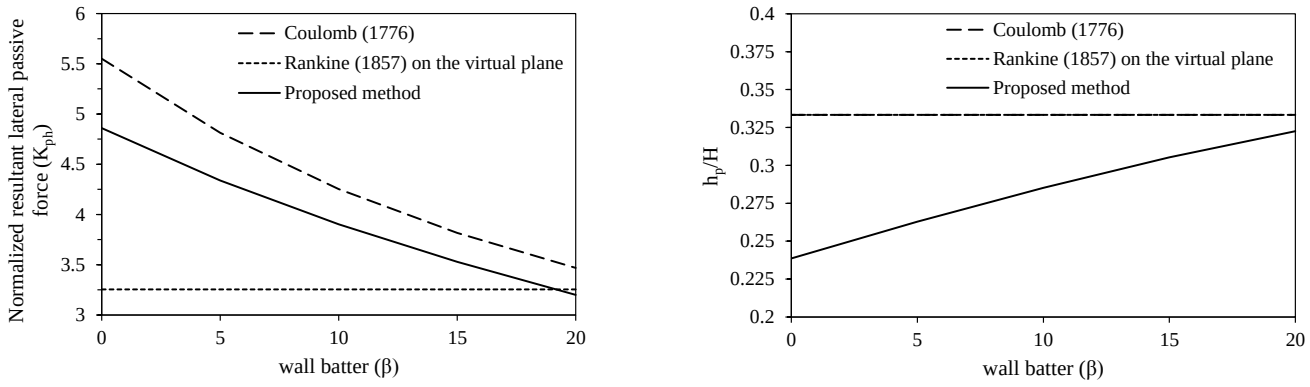

a) b)

Fig. 9. Thrust force and its application point, a) thrust force, b) application point

REFERENCES

Alqarawi, A.S., Leo, C.J., Liyanapathirana, D.S., Sigdel, L., Lu, M., & Hu, P. (2021). A spreadsheet-based technique to calculate the passive soil pressure based on the log-spiral method. Computers and Geotechnics, 130.

Cai, Y., Chen, Q., Zhou, Y., Nimbalkar, S., & Yu, J. (2017). Estimation of passive earth pressure against rigid retaining wall considering arching effect in cohesive-frictional backfill under translation mode. International Journal of Geomechanics, 17 (4), 4016093.

Cao, W., Liu, T., & Xu, Z. (2019). Calculation of passive earth pressure using the simplified principal stress trajectory method on rigid retaining walls. Computers and Geotechnics, 109, 108–116.

Chen, F., Lin, Y., & Yang, J. (2020). Passive earth pressure of narrow cohesionless backfill against inclined rigid retaining walls under translation mode. Soils and Foundations, 60 (5), 1226–1240.

Chen, F., Lin, Y., Yang, J., & Huang, M. (2021). Passive Earth pressure of narrow cohesionless backfill against rigid retaining walls rotating about the base. International Journal of Geomechanics, 21 (1), 6020036.

Chen, H., Chen, F., & Lin, Y. (2022). Slip-Line Solution to Earth Pressure of Narrow Backfill against Retaining Walls on Yielding Foundations. International Journal of Geomechanics, 22 (5), 4022051.

Dalvi, R.S. & Pise, P.J. (2012). Analysis of arching in soil-passive state. Indian Geotechnical Journal, 42 (2), 106–112.

Fang, Y.-S., Chen, T.-J., and Wu, B.F. (1994). Passive earth pressures with various wall movements. Journal of Geotechnical Engineering, 120 (8), 1307–1323.

Fang, Y.-S., Ho, Y.-C., & Chen, T.J. (2002). Passive earth pressure with critical state concept. Journal of Geotechnical and Geoenvironmental Engineering, 128 (8), 651–659.

Ghaffari Irdmoosa, K. & Shahir, H. (2019). Analytical solution for passive earth pressure of c-φ soil using principal stress rotation assumption. Journal of GeoEngineering, 14 (1), 31–39.

Jiang, M., Niu, M., & Zhang, W. (2022). DEM analysis of passive failure in structured sand ground behind a retaining wall. Granular Matter, 24 (2), 1–22.

Jun-wu, X.I.A., Guo-tao, D.O.U., & Qiong, S.U. (2019). An experiment study on the non- limit passive earth pressure of clay under different displacement modes. Journal of Southwest Jiaotong University, 54 (4), 769–777.

Kejia, W., Yu, P., & Liu, Y. (2021). Simulation of Passive Earth Pressure against Retaining Wall Considering Wall Movement Mode. In: IOP Conference Series: Earth and Environmental Science.

Khosravi, M.H., Pipatpongsa, T., & Takemura, J. (2013). Experimental analysis of earth pressure against rigid retaining walls under translation mode. Géotechnique, 63 (12), 1020–1028.

Liu, S., Xia, Y., & Liang, L. (2018). A modified logarithmic spiral method for determining passive earth pressure. Journal of Rock Mechanics and Geotechnical Engineering, 10 (6), 1171–1182.

Lu, K., Zhou, G., & Shi, K. (2021). Numerical study of 3D passive earth pressure on a rigid retaining wall in three displacement modes. Arabian Journal of Geosciences, 14 (19), 1–10.

O'Neal, T.S. & Hagerty, D.J. (2011). Earth pressures in confined cohesionless backfill against tall rigid walls—a case history. Canadian Geotechnical Journal, 48 (8), 1188–1197.

Pain, A., Chen, Q., Nimbalkar, S., & Zhou, Y. (2017). Evaluation of seismic passive earth pressure of inclined rigid retaining wall considering soil arching effect. Soil Dynamics and Earthquake Engineering, 100, 286–295.

Taylor, D.W. (1948). Fundamentals of soil mechanics. LWW, 66(2).

Terzaghi, K. (1943). Theoretical soil mechanics. John Wiley & Sons, New York.

Xu, L., Chen, H., Chen, F., Lin, Y., & Lin, C. (2022). An experimental study of the active failure mechanism of narrow backfills installed behind rigid retaining walls conducted using Geo-PIV. Acta Geotechnica, 1–18.

Xu, R., Chen, Y., Yang, Z., & Gong, X. (2002). Experimental research on the passive earth pressure acting on a rigid wall. Chinese Journal of Geotechnical Engineering-Chinese Edition, 24 (5), 569–575.

Ying, H.W., Zhang, J.H., Wang, X.G., Li, B.H., & Zhu, W. (2016). Experimental analysis of passive earth pressure against rigid retaining wall under translation mode for finite soils. Chinese Journal of Geotechnical Engineering, 38 (6), 978–986.